19th Applied Aerodynamics
Conference
11-14 June 2001 Anaheim, CA

A01-31028

AIAA 2001-2470

STUDY ON AERODYNAMIC MECHANISM OF HOVERING INSECTS

Koji Isogai*and Yasuhisa Shinmoto**

Department of Aeronautics and Astronautics

Kyushu University

6-10-1 Hakozaki, Higashiku, Fukuoka 812-8581

Japan

E-mai: isogai@aero.kyushu-u.ac.jp Key words: CFD, dragonfly

Abstract

In order to clarify the fundamental mechanism of the hovering flight of a dragonfly, the numerical simulation of unsteady viscous flow around a tandem airfoil configuration oscillating in still air has been conducted by using a two-dimensional Navier-Stokes code. It is shown that the mutual flow interactions between the fore- and hind-airfoils are playing the dominant role in generating the time mean aerodynamic force acting in the direction of the stroke plane, which is indispensable for the dragonfly to hover with the body axis horizontal. The total amounts of the lifting force and the necessary power are also estimated and shown to be very close to those estimated by other researchers. Some additional numerical simulations and discussions are also presented to explain why a true hover-fly that has, in contrast with a dragonfly, only a pair of wings can also hover with the body axis horizontal.

Introduction

Dragonfly can hover with the body axis almost horizontal[1]. The mechanism of this has not yet been well understood, though many experimental [2-4] and theoretical [5-9] investigations have been conducted so far. These theoretical studies have been concentrated on quasi-steady or unsteady aerodynamics of a single airfoil, that is, the effects of the mutual interactions of the fore and hind wings have been completely neglected. According to the experimental flow visualization study by Somps and Luttges [2], however, it has been suggested that the mutual interactions between the vortices generated by the fore- and hind-wings might be playing the dominant role in generating the hovering forces. However, further details of the vortex interactions and its correlation with the lift generation mechanism have remained to be investigated. Recently, the present authors[10] presented a numerical method using a Navier-Stokes code for investigating this mutual interaction problem. They analyzed the unsteady viscous flow around a tandem airfoil configuration at a typical span-wise station of dragonfly wings, which is oscillating in still air, by assuming the flow is locally two-dimensional. They showed that the mutual interaction is playing the essential role in generating the time mean aerodynamic force acting in the direction of the stroke plane, which is indispensable for the dragonfly to hover with the body axis horizontal. Although the basic mechanism of the hovering flight of a dragonfly was disclosed qualitatively in the analyses, there were some quantitative deficiencies. Namely, the gap between the fore- and hind-airfoils was, tentatively, assumed to be about 10 percent of the airfoil chord and the chord lengths of the fore- and hind-airfoils were assumed to be the same. In reality (*Anax parthenope julius*), the gap between the fore- and

---

* Professor, Department of Aeronautics and Astronautics. Associate Fellow AIAA.

** Research Assistant, Department of Aeronautics and Astronautics.

hind-airfoils varies from 20 percent to 140 percent chord length of the fore-airfoil depending on the span-wise stations, and the chord length of the hind-airfoil is larger than that of the fore-airfoil (100 percent ~180 percent of the fore-airfoil depending on the span-wise station). As to the airfoil motion, the amplitudes of the pitching oscillations of both the fore- and hind-airfoils were assumed to be 40 deg in upward and 10 deg in downward motions, respectively, at 80 percent semi-span station in our previous paper (see next section for the definition of the amplitude of the pitching oscillation). In reality, the larger amplitudes are taken both for the fore- and hind-airfoils by *Anax parthenope julius* [11] (the quantitative data will be given in Section III). The quantitative deficiency of the results of the analysis was that the necessary power estimated for 1g hover was about 43 percent higher than the available power for *Anax parthenope julius* which is estimated by using the empirical formula[12]. This seems to be attributed to the fact that the amplitudes of the pitching oscillations of the fore- and hind-airfoils were smaller than those measured by Azuma and Watanabe[11].

In the present paper, these quantitative deficiencies of our previous analyses have been removed. For this purpose, the original code has been improved considerably, especially, in the grid generation method to cope with the large pitch amplitudes (max. 65 deg) of the airfoil oscillations.

II. Method of Analysis

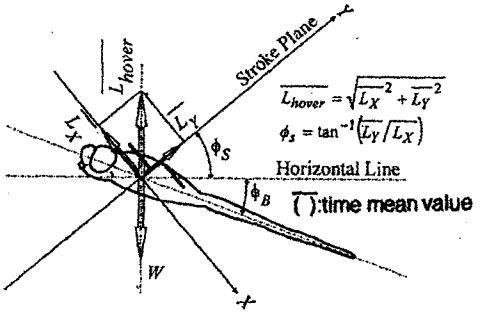

Fig. 1 Definitions of coordinates and forces

In the present analysis, we focus attention on the flow around a tandem airfoil configuration at some typical span-wise station of dragonfly wings by assuming that the flow is locally two-dimensional. In Fig. 1, the definitions of the coordinates and forces are shown. The Y-axis is taken in the direction of the stroke plane while the X-axis is taken in the direction perpendicular to the Y-axis. The fore- and hind-airfoils are assumed to be oscillating in a coupled heaving and pitching mode, where the pitching oscillation advances about 90 deg ahead of the heaving oscillation[11]. There is also some phase difference between the flapping motions of the fore- and hind-wings. That is, the hind-wing is flapping about 40 deg phase angle ahead of the fore-wing (extrapolation from the data taken by Azuma and Watanabe[11] at several non-zero flight velocities). As to the aerodynamic forces acting on the dragonfly in hovering flight condition, we define $\overline{L_Y}$ and $\overline{L_X}$ (see Fig. 1), that is, $\overline{L_Y}$ is the mean aerodynamic force (time mean value of L_Y during one cycle of oscillation) acting in the direction of the Y-axis, and $\overline{L_X}$ is the mean aerodynamic force acting in the negative direction of the X-axis. Then, the lifting force $\overline{L_{hover}}$ which balances with the body weight can be given by $\overline{L_{hover}} = \sqrt{\overline{L_X}^2 + \overline{L_Y}^2}$. The stroke plane angle ϕ_s (see Fig. 1) can be given by $\phi_s = \tan^{-1}(\overline{L_Y}/\overline{L_X})$. According to the experimental observations by Azuma and

Watanabe[11] of the dragonfly (*Anax parthehope Julius*), the value of ϕ_s for hovering is estimated as about 20 deg – 40 deg by the extrapolation from the data obtained at several finite flight velocities. In Fig. 2, the definitions of motions of the tandem airfoil configuration at some typical span-wise station of dragonfly wings are shown. The airfoil sections of the two-airfoils are assumed to be a flat-plate of zero thickness. In the figure, H_f is the displacement of the fore-airfoil in Y-direction and α_f is the angular displacement of the fore-airfoil, both at the axis of the pitch, and the similar definitions are also given to H_h and α_h for the hind-airfoil. As discussed previously, these two airfoils are assumed to be oscillating in a coupled heaving and pitching motions as follows:

For the fore-airfoil,

$$H_f = H_{f0}\sin(\omega T) \qquad (1)$$

$$\alpha_f = \alpha_{fi} + \alpha_{f0}\sin(\omega T + \phi_f) \qquad (2)$$

For the hind-airfoil,

$$H_h = H_g + H_{h0}\sin(\omega T + \Psi) \qquad (3)$$

$$\alpha_f = \alpha_{hi} + \alpha_{h0}\sin(\omega T + \Psi + \phi_h) \qquad (4)$$

where H_{f0} and H_{h0} are the amplitudes of heaving oscillations, α_{f0} and α_{h0} are the amplitudes of the pitching oscillations, and α_{fi} and α_{hi} are the mean pitch angles of the fore- and hind-airfoils, respectively, and H_g is the mean value of the heaving oscillation of the hind-airfoil. ϕ_f and ϕ_h are the phase advance angles of the pitching oscillations ahead of the heaving oscillations of the fore- and hind-airfoils, respectively. Ψ in Eqs. (3) and (4) is the phase advance angle of the heaving oscillation of the hind-airfoil ahead of the fore-airfoil. In the above equations, ω is the circular frequency of the oscillation and T is time.

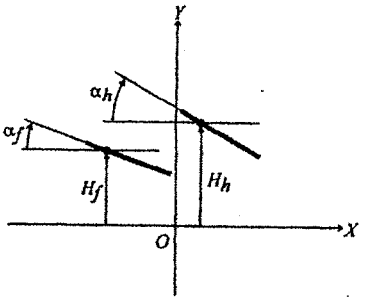

Fig. 2 Definition of airfoil motion

The compressible Navier-Stokes equations are applied for the numerical simulations of the unsteady viscous flows around the tandem airfoils whose motions are given by Eqs. (1)~(4). All the physical quantities that appear in Eqs. (1)~(4) and the Navier-Stokes equations are nondimesionalized by the maximum heaving velocity of the fore-airfoil V_f, the semi-chord length of the fore-airfoil b_f and the air density ρ (see Isogai and Shinmoto[11]). The maximum heaving velocity of the fore-airfoil is given as

$$V_f = \omega H_{f0} \qquad (5)$$

It should be noted that the similarity parameters that govern the unsteady viscous flow around the present tandem airfoil configuration in hover mode are the Reynolds number and the reduced frequency. The Reynolds number R and the reduced frequency k are defined by

$$R = (b_f V_f)/\nu \qquad (6)$$

$$k = \frac{b_f \omega}{V_f} = \frac{b_f}{H_{f0}} \qquad (7)$$

where ν is kinematic viscosity. As seen from Eq. (7), the reduced frequency k is independent of ω and equals to the reciprocal of h_{fo}. This point seems to be very important when we consider unsteady aerodynamics of the hovering flight of insect[12]. That is, if we assume the planform of the wing as rectangular, the h_{fo} which is the dimensionless flapping amplitude of the typical spanwise section is proportional to the aspect ratio of the wing. Therefore, this means that as seen from Eq. (7), the reduced frequency k is proportional to the reciprocal of the aspect ratio. Since the reduced frequency is the parameter which controls the strength of the unsteadiness of the flow, this point suggests the following interesting fact, namely, the unsteadiness of the flow around a flapping high-aspect-ratio wing is weaker than that of the low-aspect-ratio wing. As will be discussed later in this paper, this is the key point to explain why the dragonfly must utilize the mutual interactions of the fore- and hind-wings to hover and why the true hover-fly like *Syrphus ribesii* can hover by flapping only a single pair of wings.

In order to construct an appropriate grid system, a multi-domain method is employed. The physical space is divided into the four domains, namely, domain I, II, III and IV, as shown in Fig. 3a. Each physical domain, which moves and deforms with time in accord with the airfoil motion, is mapped on each corresponding domain in the computational space as shown in Fig. 3b. Each of these four domains in computational space is the rectangular region. A rectangular grid with a constant grid space is adapted to each computational domain. (Each computational domain is mapped on the corresponding physical domain at each time step by using the algebraic mapping functions.) The time differenced form of the GCL (Geometric Conservation Law)[13] coupled with the conservation form of the Navier-Stokes equations in each computational space is solved at each time step. TVD (Total Variation Diminishing) scheme[14] is employed for solving the Navier-Stokes equations. At the far-field boundaries

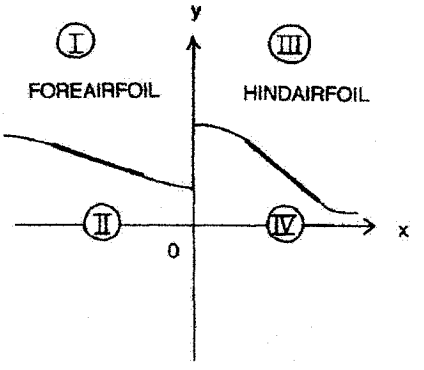

Fig. 3a Physical spaces

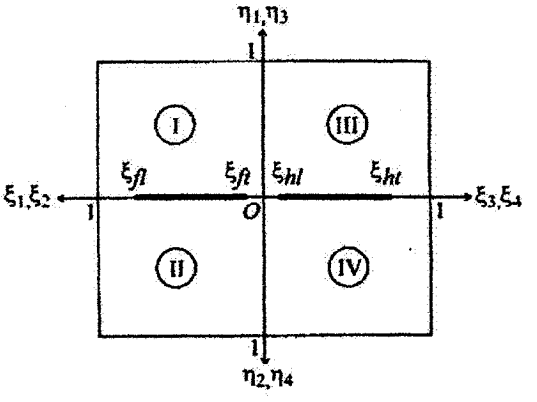

Fig. 3b Computational spaces

located 50 chord lengths away from the airfoils, the flow quantities are given by the zeroth order extrapolation from the inner points. At the boundary where the united domain of I and II and that of III and IV are overlapped, the flow quantities at the grid points of each domain should be interpolated to exchange the information since they slide each other in accord with the airfoil motions in the physical space. At

the airfoil surfaces, the no slip conditions[15] are given. Total 280x160 grid points are employed for the whole flow field. For all the flow computations, Mach number is assumed to be 0.10.

III. Dragonfly Model and Results of Simulation

In the present simulation, we take *Anax parthenope julius* as a typical example of a dragonfly. According to the observation by Azuma and Watanabe[11], the full span length of the fore-wing is 0.10m, and the aspect ratio is 10. If we assume the planform of the fore-airfoil is approximately rectangular, the chord length becomes 0.01m. The geometry of the hind-wing is a little bit different from that of the fore-wing as shown in Fig. 4. As seen in the figure, the chord length of the hind-wing is larger than that of the fore-wing. The gap between the fore- and hind-wings also varies depending on span-wise station. In the present study, we focus attention on the unsteady viscous flow around the tandem airfoil configuration at 75 percent semi-span station by assuming the flow is locally two-dimensional. At 75 percent semi-span station, the semi-chord lengths of fore- and hind-airfoils are 0.005 m and 0.0057m, respectively, and the gap between the fore- and hind-airfoils is 96 percent chord length of the fore-airfoil. Total mass of the dragonfly is $7.9x10^{-4}Kg$. As to the wing motion during hovering flight, we refer to the observation by Azuma and Watanabe[11]. Although they do not report the data for hovering flight, the data obtained for the flight velocity of 0.7m/s seems to be very close to those of the hovering flight. The flapping motions of the fore- and hind-wings, that are observed at the flight velocity of 0.7m/s, are shown in Fig. 5. The flapping frequency is 28 Hz. Thus, the amplitudes of the heaving oscillations of the fore- and hind-airfoils at 75 percent semi-span station become $H_{f0} = 0.0241m$ and $H_{h0} = 0.0241m$, and H_g becomes 0.0026 m. The maximum heaving velocity V_f, which is the reference velocity of the nondimensionalization, becomes 4.24 m/s and the reduced frequency k is 0.207 and the Reynolds number based on V_f and b_f is $1.45x10^3$. The axis of pitch is assumed to be located at 25 percent chord point for both the fore- and hind-airfoils. The amplitude of pitching oscillation is 64 deg for upward motion and 40 deg for downward motion for the fore-airfoil and 51 deg for upward motion and 24 deg for downward motion for the hind-airfoil. As

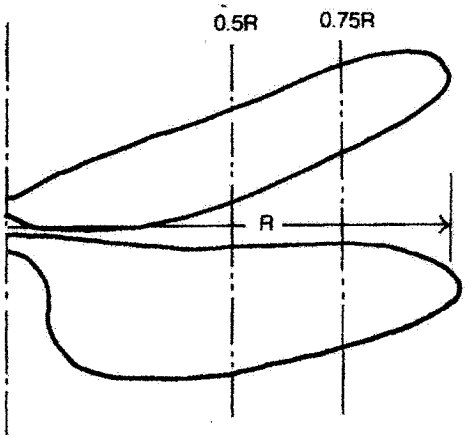

Fig. 4 Planforms of fore- and hind-wings

already mentioned, the phase advance angles ϕ_s and ϕ_h of the pitching oscillations ahead of the heaving oscillations are both 90 deg. As to the phase advance angle Ψ of the heaving oscillation of the hind-airfoil ahead of the fore-airfoil, we assume 40 deg which is obtained by extrapolation from the observed data[11] obtained at various flight velocities. We assume that α_{fi} and α_{hi} in Eqs. (2) and (4) are zero.

The numerical simulations using the Navier-Stokes code have been performed for the tandem airfoil configuration thus set. Since one of the purposes of the present study is to investigate the role of the flow interactions between the fore- and hind-airfoils, the flow simulations about the single airfoil configuration (the fore-airfoil or the hind-airfoil only) have also been performed for comparison with those for the tandem airfoil configuration.

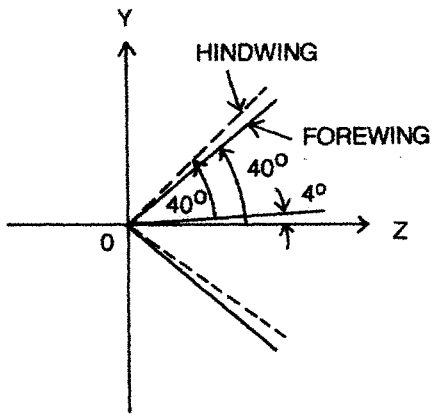

Fig. 5 Definitions of flapping motions of the fore- and hind-wings

Since the stroke-plane angle ϕ_s (see Fig. 1) plays the essential role in discussing the mechanism of the hovering flight of the dragonfly, the convergence history of ϕ_s was monitored for identifying the convergence of the computations to the periodic solution. It took more than 420 cycles of oscillation to obtain the converged value of ϕ_s for the tandem airfoil configuration, and took about 200 cycles to obtain the converged values of ϕ_s's for the single airfoil configurations. The detailed values of the time mean aerodynamic forces and the mean rate of work, that are obtained by the present simulations are as follows:

A) Tandem airfoil configuration (with interaction)

Fore-airfoil: $\overline{L_{X,f}} = 0.0868N/m$

$\overline{L_{Y,f}} = 0.0285N/m$

$\overline{W_f} = 0.375W/m$

Hind-airfoil: $\overline{L_{X,h}} = 0.0908N/m$

$\overline{L_{Y,h}} = 0.0309N/m$

$\overline{W_h} = 0.598W/m$

Sum of the fore- and hind-airfoils:

$\overline{L_X} = 0.178N/m$

$\overline{L_Y} = 0.0594N/m$

$\overline{L_{hover}} = 0.187N/m \qquad \phi_s = 18.5\text{deg}$

$\overline{W_t} = 0.973W/m$

B) Single airfoil configuration (the fore-airfoil only or the hind-airfoil only without

interaction)

Fore-airfoil: $\overline{L_{X,f}} = 0.0686N/m$

$\overline{L_{Y,f}} = 0.0092N/m$

$\overline{W_f} = 0.279W/m$

Hind-airfoil $\overline{L_{X,h}} = 0.0783N/m$

$\overline{L_{Y,h}} = 0.0074N/m$

$\overline{W_h} = 0.477W/m$

Sum of the fore- and hind-airfoils:

$\overline{L_X} = 0.147N/m$

$\overline{L_Y} = 0.0166N/m$

$\overline{L_{hover}} = 0.148N/m \qquad \phi_s = 6.4\text{deg}$

$\overline{W_t} = 0.756W/m$

The increment of $\overline{L_{hover}}$ gained by aerodynamic interaction is about 27 percent of $\overline{L_{hover}}$ obtained for the single airfoil configuration (without interaction). Especially, the increase of $\overline{L_Y}$ gained by the flow interaction, which is indispensable for the dragonfly to hover with the body axis horizontal, is about 260 percent of that of the single airfoil configuration (without flow interaction).

In Fig. 6, the variation of L_Y and L_X acting on the fore- and hind-airfoils during one cycle of oscillation are plotted by the solid line for the tandem airfoil configuration and by the dotted line for the single airfoil configuration, respectively. It can be seen in the figure that both the fore- and hind-airfoils of the tandem configuration gain L_Y and L_X, (especially L_Y) during $kt = \pi/2 \sim 1.28\pi$ when both airfoils are in downward motion. The reason for this can be seen in Fig. 7 where iso-vorticity distributions around the tandem airfoil configuration at several phases of the oscillation are plotted.

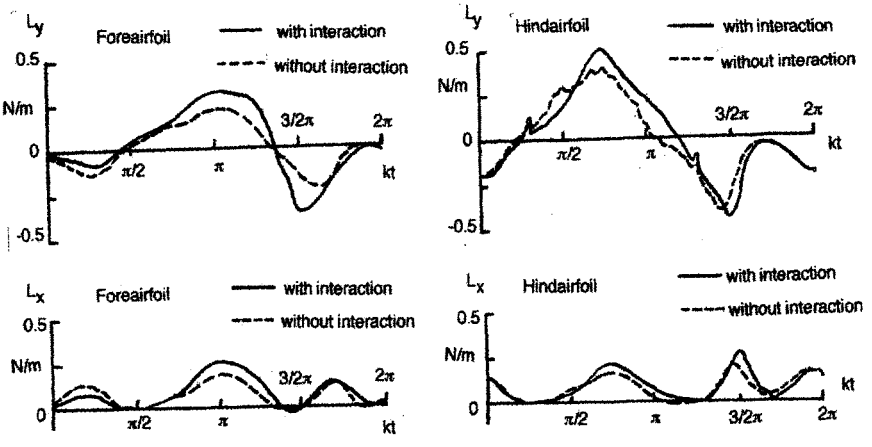

Fig. 6 Variations of L_Y and L_X during one cycle of oscillation

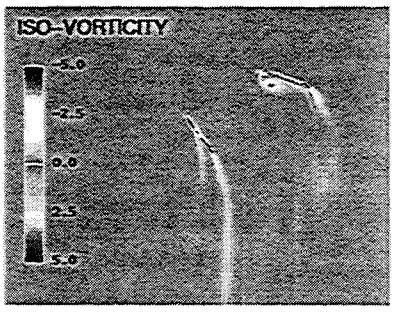

$kt = 0.17\pi$

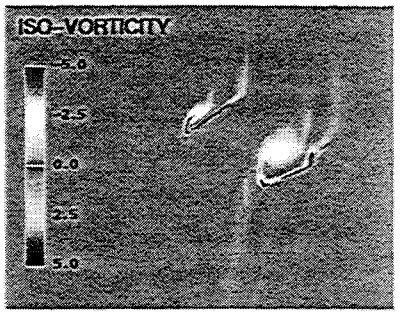

$kt = 0.83\pi$

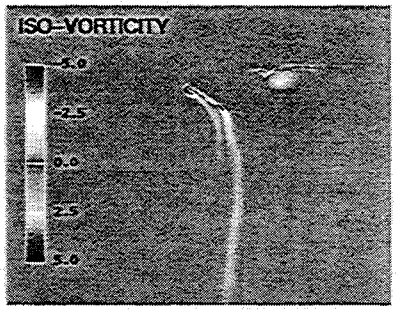

$kt = 0.33\pi$

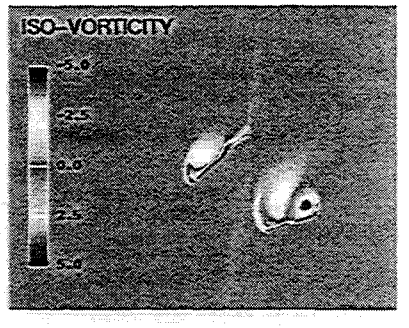

$kt = \pi$

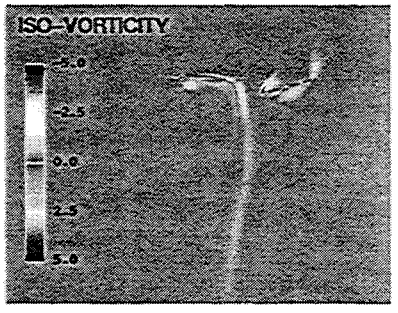

$kt = 0.50\pi$

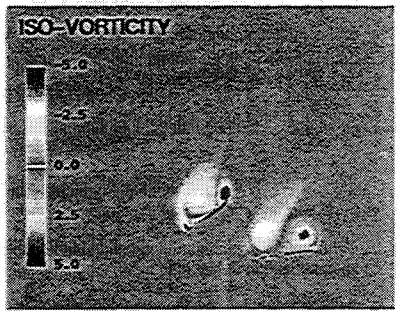

$kt = 1.17\pi$

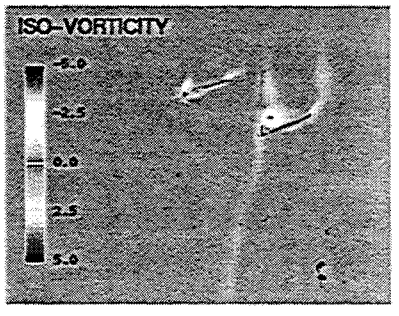

$kt = 0.67\pi$

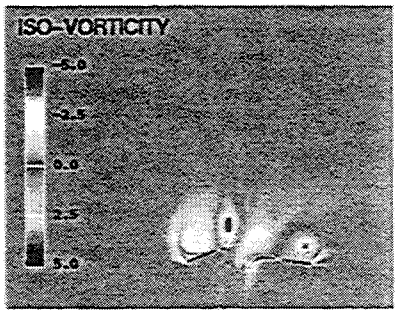

$kt = 1.33\pi$

Fig. 7 Iso-vorticity distribution around tandem airfoil configuration –continued.

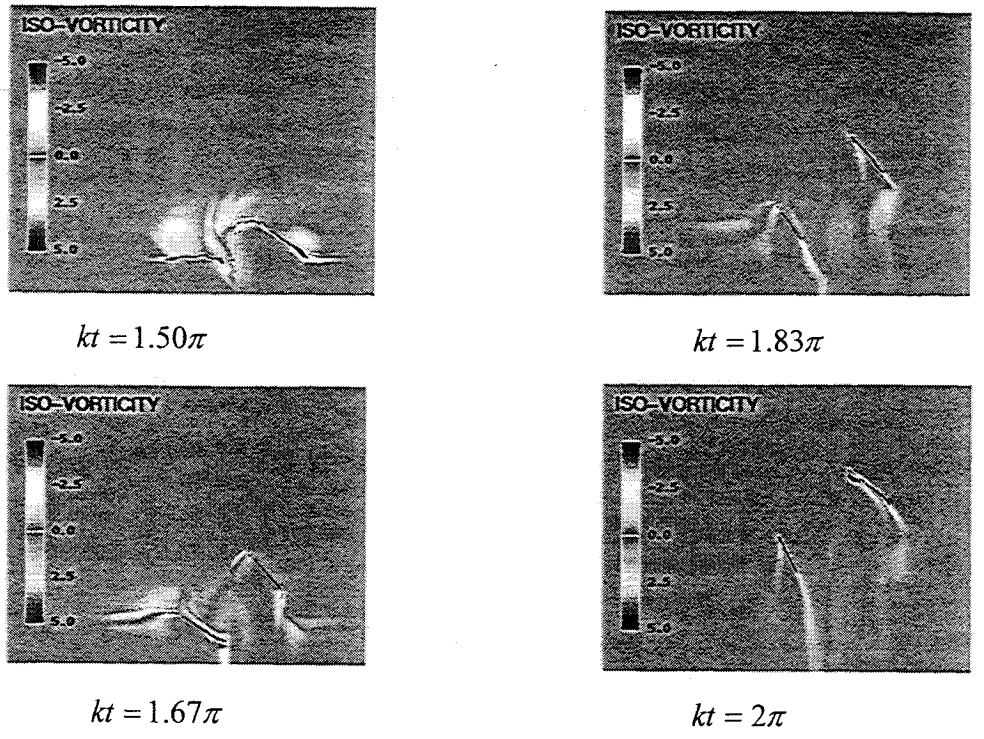

$kt = 1.50\pi$ $kt = 1.83\pi$

$kt = 1.67\pi$ $kt = 2\pi$

Fig. 7 Iso-vorticity distribution around tandem airfoil configuration –concluded.

In the process of the downward motion, the strong vortices are generated on the upper surfaces of the fore- and hind-airfoils, that produce the strong suction forces. Although the vortices on the upper surfaces also appear for the single airfoil configuration in downward motion, the strength of the vortices seems to be enhanced for the tandem airfoil configuration by the flow interactions between the two airfoils.

At this point, it is quite interesting to see whether the lifting force, $\overline{L_{hover}}$, predicted by the present numerical simulation can sustain the weight of the present dragonfly model ($7.74x10^{-3}N$). In order to estimate the total hovering force acting on the dragonfly, the span-wise distribution of $\overline{L_{hover}}$ should be given. In addition to the simulation for 75 percent semi-span station, we also performed the simulation for 50 percent semi-span station, obtaining $\overline{L_{hover}}$ =0.113 N/m. These values are plotted by the sign (o) in Fig. 8. By integrating the solid line we obtain $12.0x10^{-3}N$ as the total lifting force acting on the full span wings of the present tandem configuration. Since the weight of the dragonfly is $7.74\ x10^{-3}N$, the load factor n becomes n=1.55, and this means that the dragonfly can sustain its weight. Similarly, the necessary power for the present hovering flight can also be estimated.

In Fig. 9, the span-wise distributions of the mean rate of work, $\overline{W_t}$, are plotted. The results of the present simulation, that are obtained for 75 percent and 50 percent semi-span stations are plotted by the sign (o), respectively. By integrating the curve, we obtain the total necessary power for the full span wings of the present tandem configuration as $P_n = 0.0593W$. Using these data, the necessary power for 1g hover[11] can be estimated as $P_n' = P_n / n^{1.5} = 0.0307W$. The available power P_a of the insect is usually estimated by using the following formulae[12] (Azuma, 1992):

$$P_a / m_m = 260W / Kg$$

$$m_m / m = 1/4$$

where m_m is the muscular mass of the total mass m of an insect. When we apply these relations to the present dragonfly model, the available power is estimated to be $P_a = 0.0514W$, which is higher than the necessary power of 0.0307W estimated by the present numerical simulation. It is also easy to estimate the necessary power for 1 Kg of muscular mass, and it becomes 155 W/Kg, which is also quite reasonable value compared with 160W/Kg estimated by Wakeling and Ellington (1997) for the dragonflies, *S. sanguineum and C. splendens*.

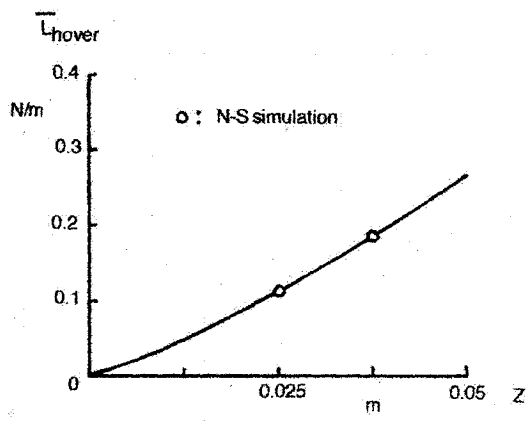

Fig. 8 Spanwise distribution fo $\overline{L_{hover}}$

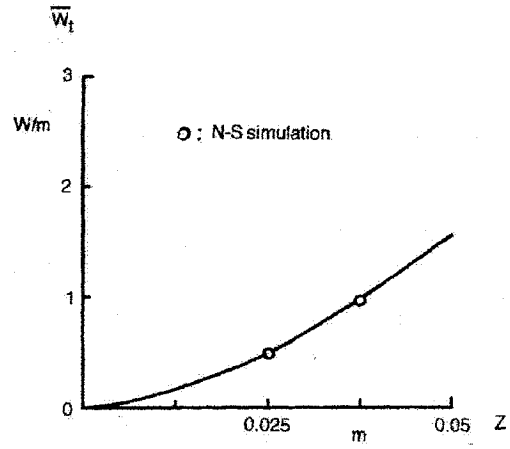

Fig. 9 Spanwise distribution of $\overline{W_t}$

IV. True Hover-Fly Model and Results of Simulation

As the conclusion of the present numerical simulations for the present dragonfly model, we have seen that the flow interaction between the fore- and hind-wings is playing the dominant role for generating the time mean force $\overline{L_Y}$, which is indispensable to keep the body axis horizontal for hovering flight. It should be noted, however, that there is a group of insects which have only a single pair of wings and can also hover with the body axis horizontal. Weis-Fogh[1] calls these insects as "True Hover-Fly". There arises a question how they generate $\overline{L_Y}$ without flow interaction, which is indispensable to hover the body axis horizontal. We should answer to this question. As already described in Section I, the major points that are different between the true hover-fly and the dragonfly are as follows: (1) the aspect ratio of the true hover-fly wing is about one half of the forewing (or hindwing) of the dragonfly, (2) the frequency of the flapping oscillation of the true hover-fly is about 170 Hz which is about six times larger than that of dragonfly, and (3) the flapping amplitude of the true hover-fly is smaller than that of the dragonfly. From the fact (1) and (3), the reduced frequency (based on the maximum flapping velocity) of the true hover-fly at the typical spanwise section is more than 2 times larger than that of the dragonfly wing. This means that the unsteady flow field around the true hover-fly wing might be quite different from that of the forewing (or hindwing) of the dragonfly even if we neglect the flow interactions between them. In this section, we will present the results of the flow simulation for a typical true hover-fly model.

For the present simulation, we take *Syrphus ribesii* [1] as a typical example of a true hover-fly model. The semispan length of the model is 0.0082 m and the chord length is 0.0031 m, and the full span aspect ratio becomes 5.3. The total mass of the model is $2.6x10^{-5}Kg$ and the frequency of oscillation is 167 Hz. The flow simulation has been performed for the airfoil motion at the 75% semispan station. The amplitude of the flapping oscillation about the body axis is assumed to be 35 deg. Therefore, the amplitude of the heaving oscillation H_0 is 0.00353m, and the semichord length b of the present 2D model is 0.00155m. The maximum velocity of the heaving oscillation, which is the reference velocity for nondimesionalizing the basic equations, is *3.70m/s*. The reduced frequency is 0.439 and the Reynolds number is 393. The amplitude of the pitching oscillation is 45deg for upward motion and 35 deg for downward motion. In Fig. 10, the variations of L_Y and L_X during one cycle of oscillation is shown. It should be noted that the relatively large values of L_Y and L_X are obtained during the aft-part of the downward motion ($kt = \pi - 3/2\pi$), where the strong leading edge

separation vortex can be seen on the upper surface of the airfoil as shown in Fig. 11. The detailed values of the time mean aerodynamic forces and mean rate of work that are obtained are as follows:

$\overline{L_Y} = 0.011N/m$, $\overline{L_X}$. $0.0173N/m$,
$\overline{L_{hover}} = 0.0205N/m$, $\phi_s = 32.4\deg$
$\overline{W} = 0.0842W/m$

The stoke plane angle of 32.4 deg means that the present true hover-fly model can hover with the body axis horizontal though it has only a single pair of wings. We can also estimate the total hovering force acting on the full span wing and the total necessary power by assuming that the spanwise distributions of $\overline{L_{hover}}$ and $\overline{W_t}$ can be expressed by the quadratic and trigonometric polynomials of Z, respectively[10]. The total time mean lifting force and necessary power thus estimated are $1.99x10^{-4}N$ and $0.819x10^{-3}W$, respectively.

. Since the total weight of the present true hover-fly model is $2.55x10^{-4}N$, the load factor becomes n=0.781. This means that the predicted aerodynamic force is about 22% less to sustain its weight. We can also estimate the necessary power for 1g hover and it becomes $1.19x10^{-3}W$. Since the available power estimated by using the empirical formula[12] is $1.69x10^{-3}W$, the necessary power estimated by the present simulation seems to be reasonable. We can also estimate the necessary power for 1Kg of muscular mass and it becomes $182.6W/Kg$ which is also reasonable compared with that estimated by other researchers[9].

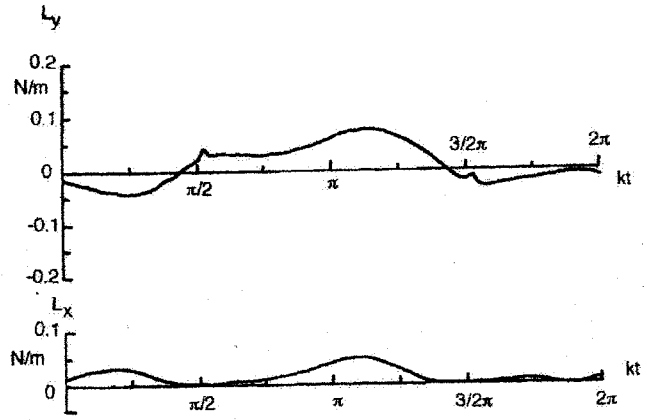

Fig. 10 Variation of L_Y and L_X during one cycle of oscillation

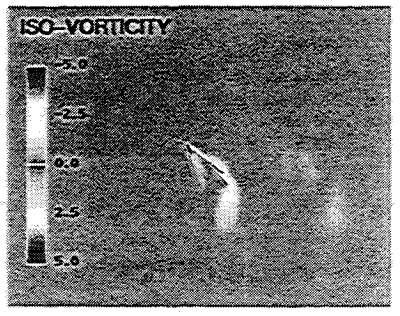

$kt = 0.17\pi$

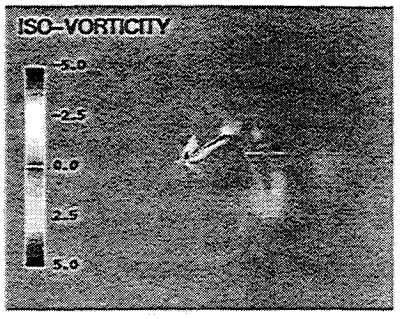

$kt = 0.83\pi$

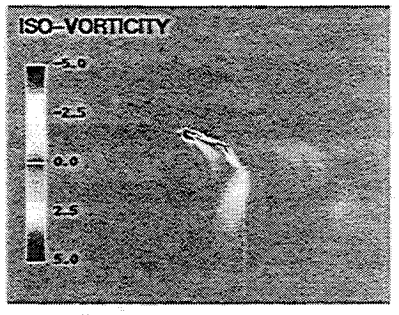

$kt = 0.33\pi$

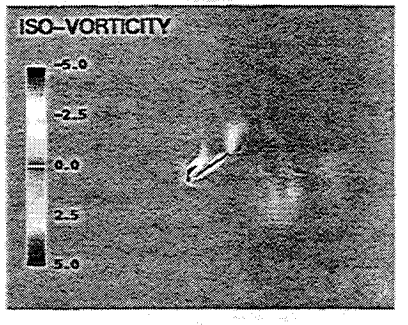

$kt = \pi$

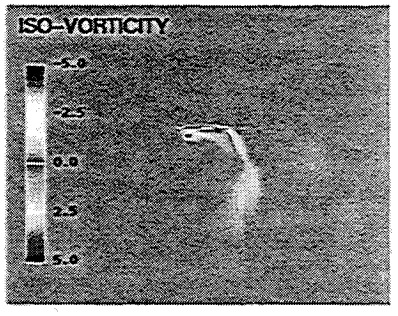

$kt = 0.50\pi$

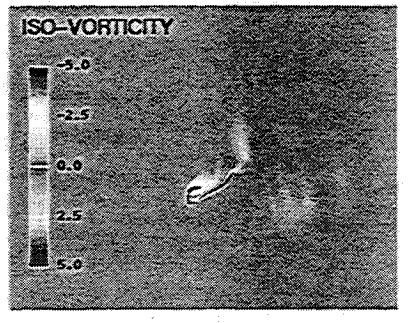

$kt = 1.17\pi$

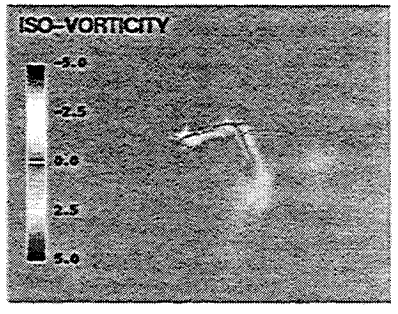

$kt = 0.67\pi$

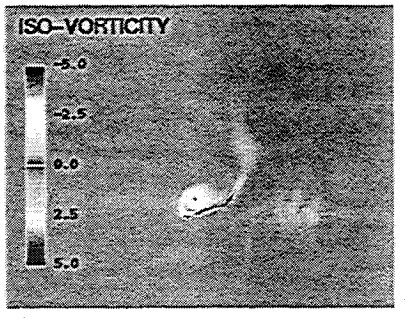

$kt = 1.33\pi$

Fig. 11a Iso-vorticity distribution around true hover-fly model –continued.

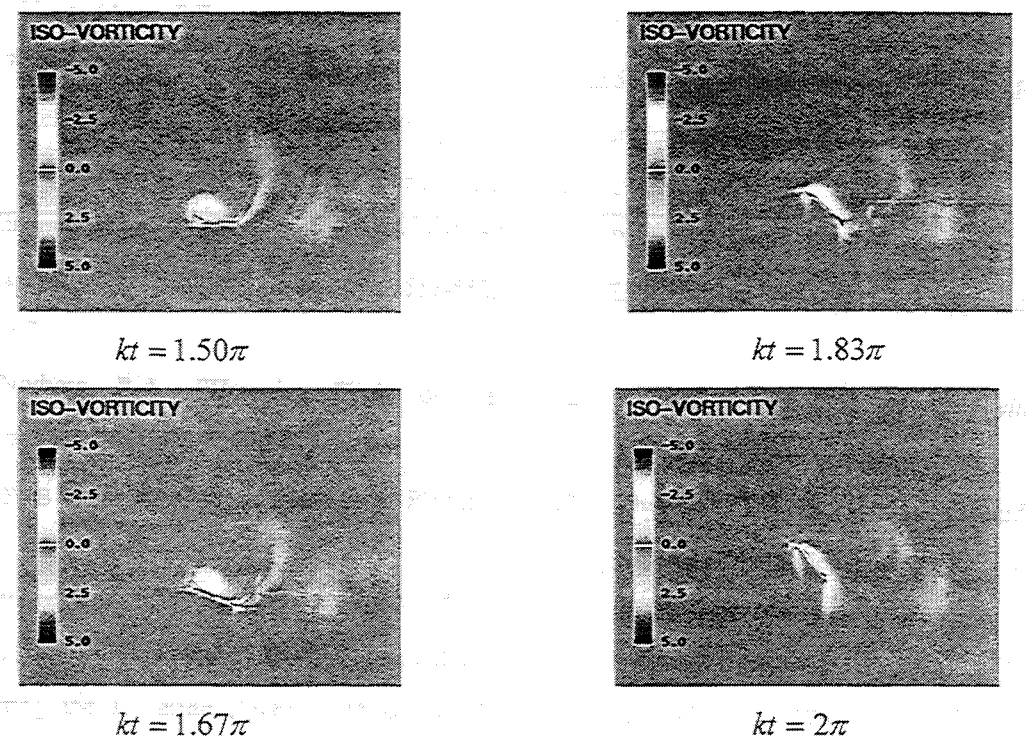

Fig. 11b Iso-vorticity distributions around true hover-fly model –concluded.

V. Conclusion

In order to clarify the fundamental mechanism of the hovering flight of a dragonfly, the numerical simulation of unsteady viscous flow around a tandem airfoil configuration oscillating in still air has been conducted by using a two-dimensional Navier-Stokes code. It is shown that the mutual flow interactions between the fore- and hind-airfoils are playing the dominant role in generating the time mean aerodynamic force acting in the direction of the stroke plane, which is indispensable for the dragonfly to hover with the body axis horizontal. The total amounts of the lifting force and the necessary power are also estimated and shown to be very close to those estimated by other researchers. Some additional numerical simulations and discussions are also presented to explain why a true hover-fly that has, in contrast with a dragonfly, only a pair of wings can also hover with the body axis horizontal.

References

1. Weis-Fogh, T.,. "Quick Estimates of Flight Fitness in Hovering Animals, Including Novel Mechanism for Lift Production," Journal of Experimental Biology, 59, pp. 169-230, 1973..
2. Somps, C., and Luttges, M., "Novel Uses of Unsteady Separated Flows," Science, Vol. 228, 14, pp. 1326-1329, 1985.

in Hover Modes," Experiments in Fluids 9, pp. 17-24, 1990.

4. Wakeling, J.M. and Ellington, C.P., "Dragonfly Flight II. Velocity, Accelerations and Kinematics of Flapping Flight," Journal of Experimental Biology, 200, pp. 557-582, 1997.
5. Norberg, R.A., "Hovering Flight of the Dragonfly *Aeschna juncea* L.," Swimming and Flying in Nature, Vol. 2, New York: Plenum, pp. 763-781, 1975.
6. Savage, S.B., Newman, B.G. and Wong, D.T.-B., "The Role of Vortices and Unsteady Effects during the Hovering Flight of Dragonflies," Journal of Experimental Biology, 83, pp. 59-77, 1979.
7. Gustafson, K. and Leben, R., "Computation of Dragonfly Aerodynamics," Computer Physics Communications, 65, pp. 121-132, 1991.
8. Gustafson, K., Jones, K., Leben, R. and McArthur, J., "Vortex Patterns, Thrust and Lift for Hovering Modes," Fourth International Symposium on Computational Fluid Dynamics, University of California, Davis, California, pp. 461-466, 1991
9. Wakeling, J.M. and Ellington, C.P., "Dragonfly Flight III. Lift and Power Requirements," Journal of Experimental Biology, 200, pp. 583-600, 1997
10. Isogai, K. and Shinmoto, Y., "Numerical Simulation and Visualization of Unsteady Viscous Flow around an Oscillating Tandem Airfoil in Hovering Mode," Proceedings of the 2nd Pacific Symposium on Flow Visualization and Image Processing 1999, PSFVIP-2, Honolulu, Hawaii, 16-19 May, 1999
11. Azuma, A. and Watanabe, T., "Flight Performance of a Dragonfly," Journal of Experimental Biology, 137, pp. 221-252, 1988.
12. Azuma, A., *The Biokinetics of Flying and Swimming*, Springer-Verlag, 1992.
13. Thomas, P. D. and Lombard, C. K., "Geometric Conservation Law and Its Application to Flow Computations on Moving Grids," AIAA J. Vol. 17, No. 10, pp.1030-1037, 1979.
14. Yee, H.C. and Harten, A., "Implicit Scheme for Hyperbolic Conservation Laws in Curvilinear Coordinates," AIAA Paper 85-1513 , 1975.
15. Steger, J.L., "Implicit Finite-Difference Simulation of Flow about Arbitrary Two-Dimensional Geometries," AIAA Journal, Vol. 16, No. 7, pp. 679-685, 1978.